Biochimica et Biophysica Acta, 1026 (1990) 93–98
Elsevier

BBAMEM 74906

Kinetic study of interaction between [^{14}C]amphotericin B derivatives and human erythrocytes: relationship between binding and induced K^+ leak

J. Wietzerbin [1], W Szponarski [2,*], E. Borowski [3] and C.M. Gary-Bobo [1,**]

[1] *Service de Biophysique, Département de Biologie, CEN Saclay, Gif-sur-Yvette,* [2] *Laboratoire de Physique et Chimie Biomoléculaire (U A CNRS No 198), Paris (France) and* [3] *Department of Pharmaceutical Technology and Biochemistry, Technical University of Gdańsk, Gdańsk (Poland)*

(Received 5 December 1989)

Key words Polyene antibiotic, Amphotericin B derivative, Antibiotic–membrane interaction, Potassium pore, (Human erythrocyte)

The relationship between polyene antibiotic binding to red cells and their membrane permeabilization was studied using two ^{14}C-labelled amphotericin B (AmB) derivatives: *N*-fructosyl AmB and *N*-acetyl methyl ester AmB. The binding kinetics of both derivatives were determined on whole red cells and ghosts. The resulting experimental points were well fitted by monoexponential functions, and the characteristic $t_{1/2}$ for both derivatives were calculated from these functions. At $2 \cdot 10^{-5}$ M, the half time $t_{1/2}$ for *N*-acetyl methyl ester AmB (30.2 min) which forms aqueous aggregates was longer than the $t_{1/2}$ for the more soluble species *N*-fructosyl AmB (4.5 min). At lower concentrations (10^{-7} M), the $t_{1/2}$ for *N*-acetyl methyl ester AmB (6.3 min) in a more solubilized form was close to that of *N*-fructosyl AmB (7.9 min). These results suggest that only solubilized species bound to red cell membranes and that disaggregation of aggregates is the limiting step in the binding process. The permeabilization of red cell membranes by *N*-fructosyl AmB, measured as intracellular K^+ leak, was not instantaneous and at 10 °C external K^+ was only detected 20 min after antibiotic addition. In contrast, binding occurs without lag time. Consequently, different mecanisms underlie binding and K^+ permeability inducement. Absorption spectroscopy data showed that bound antibiotic is located in the hydrophobic membrane interior and that this penetration of the membrane by AmB derivatives occurs without lag time. Consequently, the lag time occurring for K^+ permeability inducement would be due to some steps subsequent to binding and probably located in the hydrophobic membrane interior. This statement is further supported by the observation that the lag time is sensitive to changes in membrane fluidity as shown here by the break between 20 and 30 °C in the slope of the Arrhenius plot for the lag time, coinciding with the phase transition in red cell membranes.

Introduction

The interaction of amphotericin B with human erythrocytes as representative of mammalian cells has been frequently studied (for review see Ref 1) We recently measured the binding of four ^{14}C-labelled amphotericin B derivatives to human erythrocytes, and the results showed a simple partioning of these four derivatives between the cells and buffer, according to their lipid solubility [2] We also showed that there is no direct relationship between the partition coefficients of these derivatives and their activity as ionophores On the basis of these findings, we proposed that the differences in the permeabilizing efficiency of these derivatives are not due to binding, but to the subsequent steps leading to permeable pathway formation

The present work was undertaken in an attempt to elucidate the successive events leading to the increase in ionic permeability induced by amphotericin B derivatives

Materials and Methods

Two ^{14}C-labelled derivatives of amphotericin B *N*-fructosyl AmB and *N*-acetyl methyl ester AmB, were synthesized as previously described [2] The specific radioactivity obtained was 4 4 10^8 Bq/mM for the glycosylated compounds and 7 4 $\cdot 10^8$ Bq/mM for the acetylated compounds

* Present address INRA, BV 1540, 21034 Dijon Cedex, France
** This paper is dedicated to the memory of Professor C M Gary-Bobo, who passed away on April 2, 1989

Correspondence J Wietzerbin, Service de Biophysique, Département de Biologie, CEN Saclay, 91190 Gif-sur-Yvette Cedex, France

The chemical purity of these compounds after synthesis and their stability during storage in the solid state at −70 °C were tested by thin-layer chromatography, autoradiography and absorption spectroscopy The biological activity of the derivatives, expressed as their haemolytic activity in human red cells, was concomitantly measured

All the above tests showed that the ^{14}C-labelled compounds remained stable during storage for at least 3 months

Human erythrocytes were isolated by centrifugation at 1500 × *g* for 5 min from fresh blood samples of healthy donors Serum and buffy coat were removed, and the erythrocytes were washed three times in isotonic phosphate-buffered saline (PBS) containing 140 mM NaCl, 30 mM sucrose and 5 mM sodium phosphate (pH 7 4) This solution was used throughout this work Red cells were used within 24 h of sampling

The glycosylated and acetylated derivatives were dissolved in dimethylformamide whose final concentration in the samples never exceeded 0 5% and did not affect the erythrocytes

Kinetics of the binding of amphotericin B derivatives to red cells

For each derivative, the amount giving the desired concentration in the sample was added to a red cell suspension at 2 10^9 cell/ml (haematocrit 20%) The suspension was incubated at the desired temperature with mild shaking At different times during incubation, 2-ml aliquots were centrifuged at 1500 × *g* for 5 min and the radioactivity of the supernatants was counted The amounts of derivatives bound to red cells were calculated as described in detail previously [2]

Preparation of red cell resealed ghosts

Resealed human erythrocyte ghosts were prepared by the method of Steck [3] and the amount of ghosts in suspension was determined as the amount of membrane phospholipids, using ferrothiocyanate colorimetry [4] The same buffer solution was used as in the red cell experiments

Kinetics of binding of amphotericin B derivatives to red cell ghosts

When *N*-fructosyl AmB and *N*-acetyl methyl ester AmB bound to ghosts, the antibiotic absorption band, which in aqueous medium is centered at about 410 nm, shifted to 416 nm However, it is difficult to monitor this shifted band directly on the absorption spectrum of the whole suspension, because it is masked by the absorption band of the free antibiotic, whose amount is much greater than that of bound antibiotic [5] To subtract the contribution of free antibiotic from absorption spectrum of whole suspension, we used the following device the sample compartment of the spectrophotometer contained a quartz cuvette with ghosts in suspension plus antibiotic derivative The reference compartment contained two quartz cuvettes, the first with the ghost suspension, as in the sample cuvette, and the second, with the antibiotic derivative in buffer at the same concentration as in the sample cuvette

Obviously, the resulting differential absorption spectrum permitted the subtraction of the free antibiotic derivative contribution and monitoring in the time the appearance of the differential absorption band at 416 nm resulting from antibiotic binding to the ghost membrane In this series of experiments non-radioactive derivatives were used

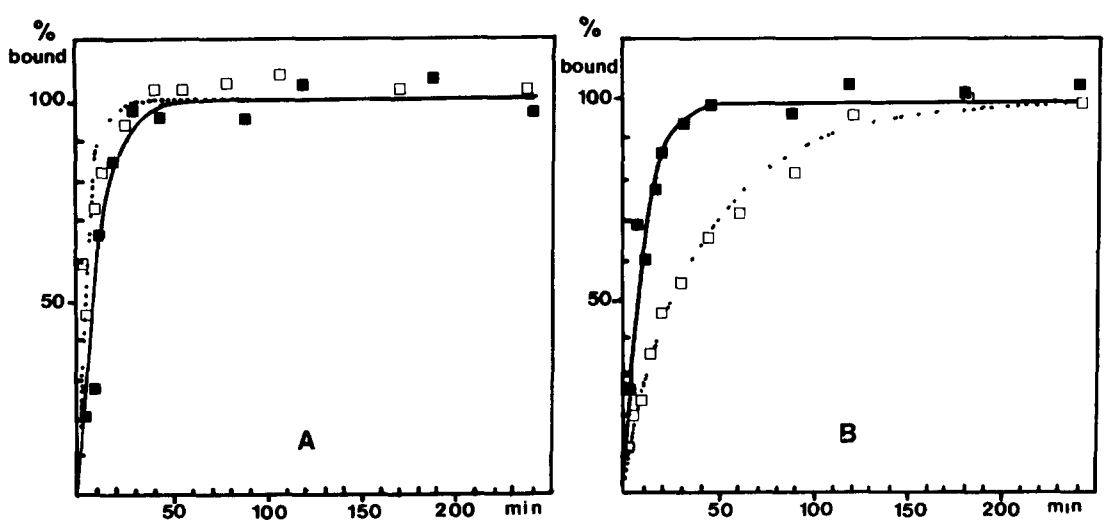

Fig 1 Binding of ^{14}C-AmB derivatives to red cells as a function of time At each time, the radioactivity fixed to 2 10^9 red cells/ml in PBS was measured and expressed as per cent of binding at equilibrium The line through the experimental points is the theoretical monoexponential curve (A) ■, *N*-fructosyl AmB 2 10^{-5} M, □, *N*-fructosyl AmB 10^{-7} M (B) □, *N*-acetyl methyl ester AmB 2 10^{-5} M, ■, *N*-acetyl methyl ester AmB 10^{-7} M

Kinetic of induction of permeability to K^+

A selective K^+ electrode (F 2312 K Radiometer Copenhagen) was introduced into the same red cell suspension containing 2 10^9 red cells/ml as the one used for the binding experiments When the recorded signal has stabilized, the antibiotic was added and K^+ release continuously monitored Lastly, the red cells were completely haemolysed by osmotic shock and their total potassium content was then measured

Results

Binding of ^{14}C-labelled amphotericin B derivatives to red cells

Fig 1 shows typical kinetics for the binding at 37 °C of *N*-fructosyl AmB (1A) and *N*-acetyl methyl ester AmB (1B) to red cells Two concentrations of each derivative were used, 10^{-7} M and $2 \cdot 10^{-5}$ M

The experimental data were well fitted by monoexponential functions (dotted and full lines) For *N*-fructosyl AmB (Table I) the calculated characteristic $t_{1/2}$, i e the times required for 50% binding saturation, were similar at 10^{-7} M and $2 \cdot 10^{-5}$ M (7.9 vs 4 5 min) However, for *N*-acetyl methyl ester AmB, these $t_{1/2}$ were concentration-dependent and very different (Table I) since at 2 10^{-5} M, $t_{1/2}$ was 30 2 min, but at 10^{-7} M it was only 6 3 min, i e in the range of $t_{1/2}$ values for *N*-fructosyl AmB This concentration-dependence might be due to the much lower water-solubility of *N*-acetyl methyl ester AmB as compared to that of *N*-fructosyl AmB As we previously showed [2], *N*-fructosyl AmB remains 'soluble' (non sedimentable at $1000 \times g$) at both 10^{-7} and 2 10^{-5} M while 60% of *N*-acetyl methyl ester AmB at 2 10^{-5} is aggregated in sedimentable form

It therefore appears that this aggregation in aqueous medium, markedly reduced the rate of antibiotic binding to red cells compared to the binding kinetics of the soluble 'monomer' form

Fig 2 shows the effect of temperature on the binding kinetics of *N*-fructosyl AmB at a final concentration of

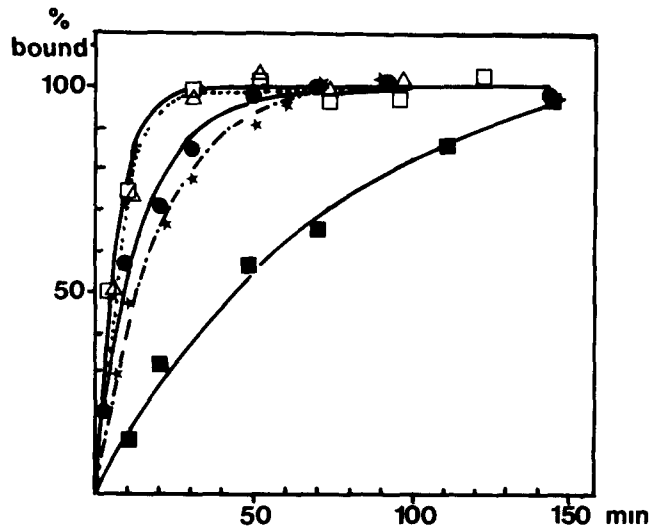

Fig 2 Binding of ^{14}C-*N*-fructosyl AmB (2 10^{-6} M) to 2 10^9 red cells/ml in PBS as a function of time and at different temperatures □, 37 °C, △, 30 °C, ●, 20 °C, *, 10 °C, ■, 5 °C

2 10^{-6} M Experiments were done at 37, 30, 20, 10 and 5 °C Within this temperature range, saturation levels did not differ significantly, and the bound/free antibiotic ratio was 0 3, as reported previously [2]

At all temperatures, the experimental points were well fitted by a single exponential From the theoretical curves in Fig 2, we calculated the time required to reach 50% binding saturation ($t_{1/2}$, Table II, line 2) at each temperature

Binding of AmB derivatives to red cell ghosts

The study of AmB derivative interaction with resealed ghosts permitted the monitoring of antibiotic interaction with erythrocyte membranes using absorption spectroscopy As this study is difficult with whole red cell suspensions due to the strong absorption capacity of haemoglobin, the resealed ghosts were used This method allows us to make measurements faster than in the radioactive method previously depicted

TABLE I

The $t_{1/2}$ values of binding experiments on 2 10^9 red cells/ml in PBS buffer

^{14}C-*N*-fructosyl AmB (*N*-F AmB) and ^{14}C-*N*-acetyl methyl ester AmB (*N*-A MeO AmB) were used at two differents concentrations 10^{-7} M and 2 10^{-5} M at 37 °C The $t_{1/2}$, the time (min) required for 50% binding saturation was obtained by radioactivity counting as described in Materials and Methods

Concentration	$t_{1/2}$ (min)	
	N-F AmB	*N*-A MeO AmB
10^{-7} M	7 9	6 3
2 10^{-5} M	4 5	30 2

TABLE II

Binding and induced K^+ leak of ^{14}C-N-fructosyl AmB (2 10^{-6} M) on 2 10^9 red cells/ml

Experiments were done at 5, 10, 20, 30 and 37 °C The 2nd line ($t_{1/2}$) shows the $t_{1/2}$ for the antibiotic binding The 3rd line shows the lag time preceding the onset of the K^+ release from red cells induced by the antibiotic derivative The last line is the amount of bound antibiotic derivative at the end of the lag time, expressed as per cent of the binding at equilibrium

Temperature (°C)	5	10	20	30	37
$t_{1/2}$ (min)	53 8	13 6	10 0	5 2	4 5
Lag time (min)	28	20	12	4	1
Binding at the end of the lag time (%)	30 3	64 0	56 3	54 1	14 2

TABLE III

Position of absorption band (nm) of AmB derivatives in different solvents

ϵ, dielectric constant

Solvent	ϵ [a] (10 °C)	Band position (nm)
Methanol	37 4	408
Propanol	20 3	410
Octanol	11 3	412
Chloroform	5 0	418

[a] Handbook of chemistry and physics 67th edition

The basal leak of K^+ from ghosts was higher than from whole cells This fact prevents us from measuring simultaneously binding and K^+ permeability as was possible with radioactive derivatives on whole red cells

In aqueous solution, the absorption band for Amphotericin B derivatives is centered at 409 nm, which is characteristic of the monomeric form of antibiotic in aqueous medium [5] Here, however, addition of red cell ghosts altered this band, as a shoulder appeared at 416 nm

After incubation with antibiotic, the ghosts were sedimentated by centrifugation at 17000 × *g* for 10 min and the pellet was resuspended in antibiotic-free buffer The absorption spectrum recorded within the minute following resuspension showed that the shoulder previously observed at 416 nm became the principal absorption band and the conversely, the band previously observed at 409 nm became the shoulder This shows that the absorption band centered at 416 nm was due to membrane-bound antibiotic

To better define the environment of this antibiotic, we investigated the dependence of the position of the antibiotic absorption bands on the polarity of the medium Absorption spectra of amphotericin B derivatives in several organic solvents of different polarity were recorded As shown in Table III, the position of the antibiotic absorption bands was dependent on solvent polarity, expressed here as the relative dielectrical constant.

We found that, with the decrease in polarity reflected by the decline in the dielectric constant, the absorption band approached 416 nm Consequently, it may be assumed that the membrane bound antibiotic is in an environment with dielectric constant between 5 and 10 Only the hydrophobic membrane interior can have such an apolar medium. An absorption band at 416 nm is therefore characteristic of antibiotic molecules which have penetrated into the membrane's hydrophobic interior

Fig 3 shows the optical density of the absorption band at 416 nm versus time At $t = 0$ *N*-fructosyl AmB (■) or *N*-acetyl methyl ester AmB (●) was added to a suspension of 2 10^8 ghosts/ml at a final concentration

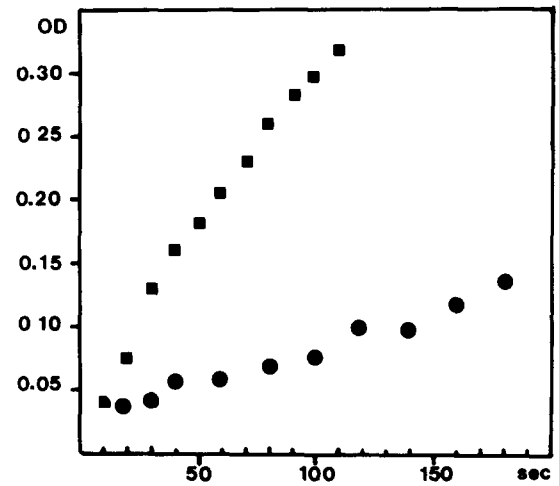

Fig 3 Binding of AmB derivatives to red cell ghosts at 10 °C as a function of time At $t = 0$, 4 10^{-6} M of antibiotic was added to 2 10^8 red cell ghosts/ml in PBS solution OD, optical density at 416 nm, ■, ^{14}C-*N*-fructosyl AmB, ●, ^{14}C-*N*-acetyl methyl ester AmB

of 4 10^{-6} M This concentration was the minimal required to observe the band at 416 nm A low temperature of 10 °C, was chosen in order to slow down the binding kinetics The binding of both antibiotics started almost instantaneously without any lag time The band at 416 nm could be detected within 10 s after antibiotic addition The kinetic of the binding of both AmB derivatives were different *N*-fructosyl AmB bound faster than *N*-acetyl methyl ester AmB As previously stated, this may be due to aggregation of *N*-acetyl methyl ester AmB About 30% of this compound aggregates at 4 10^{-6} M, while *N*-fructosyl AmB is monomeric [4]

Kinetic of potassium release

Fig 4 shows the curves recorded for the percent of total K^+ released versus time At $t = 0$, *N*-fructosyl AmB was added at a final concentration of 2 10^{-6} M

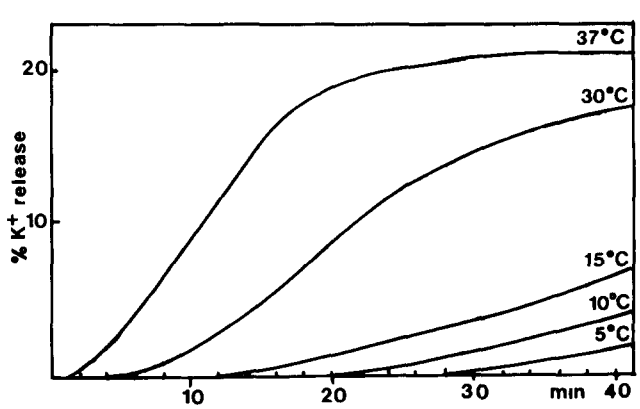

Fig 4 Kinetics of K^+ release from red cells induced by AmB derivatives At $t = 0$ ^{14}C-*N*-fructosyl-AmB (2 10^{-6} M) was added to 2 10^9 red cells/ml in PBS The percent of K^+ release in relation to the total red cell K^+ content was followed with a K^+ selective electrode

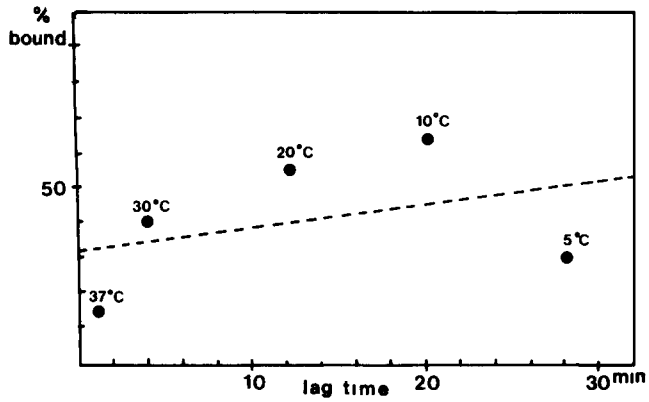

Fig 5 Percent of ^{14}C-*N*-fructosyl-AmB bound to 2 10^9 red cells/ml at the end of the lag time for K^+ release vs the lag time at each temperature Dotted line is the regression line with $r = 0\,31$ (not significant, $P > 0\,1$)

to red cell suspension (2 10^9 cells/ml) Experiments were run at 5, 10, 20, 30 and 37 °C

The antibiotic action was not instantaneous and a lag time for K^+ appearance in the outside solution was measured at all temperatures (Table II, line 3) The electrode sensitivity allowed us to measure at least 1% of the total K^+ content of red cells The error in the lag time in the least favorable situation (at 5 °C) was $< 0\,1$ min

At 37 °C, the effect of *N*-fructosyl AmB on K^+ leak was very rapid, since 1 min after its addition, K^+ was detected in the solution In contrast, at 5 °C, the K^+ leak was only detected after 28 min

The $t_{1/2}$ of binding experiments were far less temperature dependent than the lag time, especially in the range of 10–37 °C In this range, binding $t_{1/2}$ increased only 3-fold (from 4 5 to 13 6) whereas the lag time increased 20-fold (from 1 to 20) These meaningful differences substantiate the idea that different mechanisms underlie binding and K^+ permeability inducement

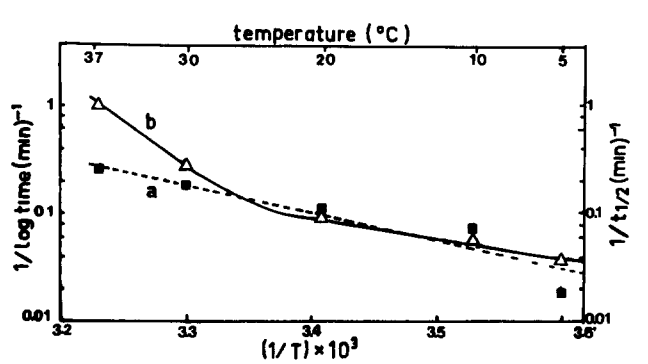

Fig 6 (a) Arrhenius plot for the rate of binding of 2 10^{-6} M of ^{14}C-*N*-fructosyl-AmB to 2 10^9 red cells/ml The inverse of the half time of binding ($1/t_{1/2}$) as a measure of binding rate was traced in function of the inverse of the absolute temperature (■) (b) Arrhenius plot for the lag time of K^+ release induced by 2 10^{-6} M of ^{14}C-*N*-fructosyl-AmB on 2 10^9 red cell/ml The inverse of lag time as a measure of K^+ permeabilization rate was traced versus the inverse of the absolute temperature (△)

Moreover, there was no correlation between the amount of *N*-fructosyl AmB bound and the time when K^+ appeared in the external solution after the *N*-fructosyl AmB addition (lag time) This is confirmed by the graph in Fig 5 in which the per cent of bound *N*-fructosyl AmB at the end of the lag time (table II, last line) was plotted against the lag time for each temperature The correlation coefficient of 0 36, which was not significant ($P > 0\,1$), indicates the absence of a correlation between binding and K^+ leak (the dotted line is the regression line)

These findings allow us to state that different mechanisms underlie binding and K^+ permeability inducement

To examine more closely the dependence between K^+ permeability inducement and antibiotic binding, Arrhenius curves was plotted (Fig 6), using the data of Table II (3rd and last line) In curve b, a semilog plot of the inverse of the lag time for red cell K^+ release (as a measure of the permeabilization rate) was traced as a function of the inverse of the absolute temperature Curve 6a shows an Arrhenius plot for the inverse of $t_{1/2}$ of binding as a measure of the binding rate Fig 6b shows a break of the slope between 20 and 30 °C In this range, a characteristic modification in membrane fluidity was reported [6] In contrast to the Arrhenius plot for the lag time in curve b, the Arrhenius plot for the rate of binding to red cells (curve a) showed no breaks, and a straight line could be drawn through the experimental points

Discussion

Antibiotic binding

The experiments depicted in Fig 1 show that the kinetics of the two amphotericin B derivatives *N*-fructosyl AmB and *N*-acetyl methyl ester AmB, were well described by a monoexponential curve This behaviour is characteristic of a two-compartment system consisting of the cell membrane and buffer, leading to a partitioning equilibrium in accordance with previous findings [2]

One of the salient features of polyene antibiotics is their amphiphilic character The existence of hydrophobic and hydrophilic moieties is responsible for their ionophoric and physicochemical properties This amphiphilic character induces the self association of the molecule that gives aggregates in aqueous solution These aggregates were detected by circular dichroism [5] and by simple centrifugation experiments on radiolabelled derivatives [2] These experiments showed that while *N*-fructosyl AmB did not form sedimentable aggregates up to a concentration of 2 10^{-5} M, 40% of

N-acetyl methyl ester AmB formed aggregate at 2 10^{-5} M but behaved like *N*-fructosyl AmB at 10^{-7} M

The experiments depicted in Fig 1 showed that the $t_{1/2}$ values of binding experiments were similar for the three 'solubilized' forms of antibiotic, whereas they were higher for the non soluble, aggregated form, i e, the binding kinetics were far slower

It can therefore be assumed that the aggregate form of antibiotic binds slower or not at all to membranes, and that the desaggregation of such aggregates into either smaller aggregates or even monomeric forms of antibiotic must precede binding and might therefore be the limiting step in the binding process

The difficulty of aggregate to bind to membranes is not surprising In aqueous medium, aggregate formation favours interaction among hydrophobic polyene chains and exposes the hydrophilic regions to the aqueous medium However, this conformation is thermodynamically unfavourable to penetration into the hydrophobic interior of the membrane Therefore, such penetration requires previous disaggregation which seems to be the limiting step in binding kinetics

The data from absorption spectroscopy show that bound antibiotic penetrated into the hydrophobic membrane interior The onset of membrane penetration was almost instantaneous, i e without any lag time as shown in Fig 4 This might be due to the penetration into the membrane matrix of the monomeric form of antibiotic which is always present at equilibrium with the aggregate Consequently, the less aggregated *N*-fructosyl AmB penentrated the membrane hydrophobic matrix at higher rate than the more aggregated *N*-acetyl methyl ester AmB

The lower binding $t_{1/2}$ at higher temperatures might be due to the increase of the antibiotic diffusion coefficient D in water The expected $D(37\,^\circ C)/D(5\,^\circ C)$ ratio is about 2 5 [7], which is lower than the $t_{1/2}(5\,^\circ C)/t_{1/2}(37\,^\circ C)$ of about 12 obtained here ($t_{1/2}$ is in inverse proportion to D) Therefore mechanisms other than a simple increase of antibiotic diffusion in water with temperature might be implicated in the observed decrease of $t_{1/2}$ One possible factor which might account for this behaviour is the increased desaggregation at higher temperatures causing the increase in the concentration of the penetrating smaller aggregate or monomeric species

K^+ release

At 10 °C, membrane permeabilization by *N*-fructosyl AmB as measured by K^+ release, was delayed, since K^+ was detected with a lag time of 20 min, even though the antibiotic had penetrate the membrane very fast, within as little as 10 s, with practically no lag time Consequently, the lag time is due to some event which occurs after antibiotic binding and penetration into the membrane

The lag time for K^+ permeabilization is temperature dependent when T increase, the lag time decrease This effect may be ascribed to the increase in membrane fluidity which might affect the time required for the antibiotic to build up permeable structures More, Arrhenius plot shows a brekdown of *N*-fructosyl-AmB permeabilizing efficiency between 20 and 30 °C In this temperature range, a transition phase is observed in erythrocyte membranes [6]

Taking together, these observations suggest that the step subsequent to binding and leading to K^+ leak is located in the membrane matrix and is sensitive to the membrane physical state

In contrast, the Arrhenius plot for $t_{1/2}$ values of *N*-fructosyl AmB binding did not exibit any discontinuity and can be fitted by a single straight line These results show that unlike potassium permeation, binding is insensitive to phase transition in the membrane

Two majors steps in the interaction of AmB derivatives with red cells have been described in this paper The first one, occurring in the aqueous medium is the dissociation of antibiotic aggregates giving the monomers which can quickly bind to the membrane The second one, located in the membrane hydrophobic interior, is strongly dependent on membrane physical state and consists in the diffusion of bound antibiotic leading to the membrane permeabilisation However, is not clear whether the kinetics of 'pore' formation is limited by the diffusion of antibiotic in the lipid matrix and/or by the reorganization of antibiotics molecules to build permeable K^+ pathway Further studies are required to provide additional information concerning this issue

References

1 Bolard, J (1986) Biochim Biophys Acta 864, 257–304
2 Szponarski, W, Wietzerbin, J, Borowski, E, Gary-Bobo, C M (1988) Biochim Biophys Acta 938, 97–106
3 Steck, T L (1974) Methods Membr Biol 2, 245–281
4 Marshall Steward, J H (1980) Anal Biochem 104, 10–14
5 Mazerski, J, Bolard, J, Borowski, E (1982) Biochim Biophys Acta 719, 11–17
6 Galla, H J, Luisetti, J (1980) Biochim Biophys Acta 596, 108–117
7 Tanford, C (1967) in Physical Chemistry of Macromolecules, John Wiley and Sons, New York